DOI: 10.5516/NET.2011.43.3.309

〈Technical Note〉

BEHAVIORS OF MOLYBDENUM IN UO_2 FUEL MATRIX

YEONG-KEONG HA*, JONG-GOO KIM, YANG SOON PARK, SOON DAL PARK, and KYUSEOK SONG
Korea Atomic Energy Research Institute
1045 Daedeokdaero, Yuseong, Daejeon, 305-353, Korea
*Corresponding author. E-mail : nykha@kaeri.re.kr

Received August 16, 2010
Accepted for Publication February 07, 2011

Molybdenum is the most abundant fission product since its fission yield is equivalent to that of xenon, and it has a very special role in the chemistry of nuclear fuel because it influences the oxygen potential of UO_2 fuel. In this study, the distribution of molybdenum in spent UO_2 fuel specimens with 33.3, 41.0 and 57.6 GWd/tU burnup was measured by a LA-ICP-MS system and the reproducibility of the measured data was obtained. The Mo distribution was almost constant along the radius of a fuel except an increase at the periphery of the fuel. It showed a drop in reproducibility with relatively high deviation of measured values for the highest burnup fuel. To explain this, the state of molybdenum in a UO_2 matrix and its effect on the oxidation behavior of UO_2 were investigated. The low reproducibility was explained by the segregation of molybdenum, and the inhibition of oxidation by the molybdenum was also observed.

KEYWORDS : Molybdenum, Uranium Dioxide, Distribution, Chemical State, Oxidation

1. INTRODUCTION

The distribution of fission products in a spent nuclear fuel is important to assess the operational performance and safety of the fuel, and also the long-term behavior of spent fuel after its final disposal. The fission products could be categorized by groups: elements that form solid solutions with UO_2, those that precipitate into a UO_2 matrix in the forms of oxides or metals, and volatile elements [1, 2]. Among the elements that precipitate into a UO_2 matrix, molybdenum is the most abundant fission product since its fission yield is equivalent to that of xenon [2, 3]. It is well known that molybdenum belongs to two categories at a time [4], either dissolving in the matrix or forming precipitates. It exists as precipitates mainly located in voids, bubbles and grain boundaries [3, 5, 6], as well as a solid solution in UO_2 spent fuel. In addition, it has a very particular role in the chemistry of nuclear fuel because the oxygen potential of Mo/MoO_2 buffers the oxidation of uranium dioxide [2, 3, 7] when exposed to an oxidizing atmosphere. If oxygen potential is high enough ($\Delta G_{O2} > \Delta G_{Mo}$), Mo may exist as an oxide form (MoO_2) which causes a depletion of metallic precipitates. Therefore, the chemical state of molybdenum could indicate the fuel oxidation state. Nicoll et al. [6] reported the location and charge state of Mo throughout the UO_2 lattice, and it was concluded through computer simulation that molybdenum would be present as neutral atoms in a Schottky defect (trivacancy sites for hypostoichiometric UO_2 and di- and trivacancy sites in stoichiometric UO_2).

In this work, the distribution of $^{100}Mo/^{235}U$ in spent nuclear fuels and the reproducibility of its measured values were obtained. In addition, the effect of molybdenum on a spent nuclear fuel and its oxidation behavior were investigated for a more precise understanding in order to explain the comparatively lower reproducibility for higher levels of molybdenum content.

2. EXPERIMENTAL

2.1. Measurements of ^{100}Mo Distributions in Spent Fuels

Spent nuclear fuels originating from the Yeonggwang-2 nuclear reactor were used as test specimens (33.3, 41.0 and 57.6 GWd/tU). Axial slices of 3 mm in height and 1 mm in thickness were cut along the diameter of nuclear fuel pellets to produce samples that included both the core of the pellet and a cladding. The specimens were embedded in epoxy resin and then polished well in a post-irradiation examination (PIE) facility. The time after discharge to measurement was ca. 3 years for all specimens. For the measurement of fuel burnup, the spent fuel specimens were analyzed by a chemical dissolution method as described in our previous paper [8]. The prepared sample specimens were transferred into the ablation chamber in a shielded glove box for $^{100}Mo/^{235}U$ isotope ratio measurements by laser ablation inductively

coupled plasma mass spectroscopy (LA-ICP-MS). Sampling was carried out using a Q-switched Nd:YAG laser at 266 nm. The laser was operated at 45% laser power (4mJ at 100%) with a 10Hz repetition rate and a 2s sampling time. The ablated particles were carried to the plasma of the ICP-MS system through a PVC tube. The ICP-MS system was optimized at maximum ion intensity for ^{238}U. The operating conditions of the LA-ICP-MS system are summarized in the previous paper [8].

2.2. Preparation and Characterization of UO_2 with Molybdenum Additives

A mixed oxide of uranium and molybdenum was prepared by a powder mixing technique, which is most widely used for the preparation of ceramic samples. The mixed oxide specimens were prepared from U_3O_8 and MoO_2 powder (Aldrich, 99%). To raise homogeneity, the weighed powders were thoroughly mixed and were ground for 30 minutes to provide a small particle size and to maximize the contact area of the two components. The mixed powders were compacted at 2 ton/cm^2 for 15 seconds, and were sintered in a tubular furnace for 12 hours at 1700ºC and then annealed for 12 hours at 1200ºC under a hydrogen atmosphere. The compositions of the prepared pellets as calculated from the ratios of the weighed powders are listed in Table 1.

Visual inspection of the prepared pellets and a compositional analysis of points were performed using an electron probe micro analyzer (EPMA, JXA-8600, JEOL). To identify the phases present in the prepared urania and to get information about its structural changes in the presence of molybdenum additives, X-ray diffraction spectra were obtained in the range of 2θ value from 20º to 90º with a Siemens D5000 X-ray diffraction (XRD) system. A Cu Ka line was used and filtered through Ni foil (beam current 40 mA at 40 kV). To identify compounds from the XRD spectrum, Joint Committee for Powder Diffraction Standards (JCPDS) files were used as a finger-print method for assigning the detected phases. The lattice parameters of spent fuel were calculated using the TOPAS program (Pawley fitting method, BRUKER-AXS).

Table 1. Compositions of Cations in Molybdenum-added Uranium Dioxide

Sample	U, atom%	Mo, atom%
1	100	0
2	99	1
3	98	2
4	96	4
5	92	8
6	85	15

3. RESULTS AND DISCUSSION

3.1 Distribution of ^{100}Mo in UO_2 Spent Fuels

The specimens used in this work are the same as those described in our previous paper [8]. Sampling of prepared spent fuel specimens was carried out using a Q-switched Nd:YAG laser at 266 nm with intervals varying from 500 μm around the pellet center, to 200 μm to 300 μm in the middle, and finally with 100 μm intervals in the pellet periphery. The ablated particles were carried to the plasma of the ICP-MS system by Ar carrier gas, and they were then ionized and analyzed using the ICP-MS system. Molybdenum has an atomic number of 42 and seven stable isotopes, mass numbers 92, 94, 95, 96, 97, 98 and 100. ^{100}Mo was measured among all these. The possible isobaric interference of the mass 100 in spent fuels is from ruthenium at m/q 100. The isotope ratios of $^{100}Mo/^{235}U$ from the center to the pellet outer surface were determined by using the peak areas of each isotope. Fig. 1 shows the distribution of ^{100}Mo to ^{235}U as a function of the distance from the pellet outer surface. Since the diameter of a fuel pellet is about 8 mm, around 4,000 μm in the x-axis of the figure corresponds to the pellet center. As can be observed, Mo content is constant in the center of the pellet and it is increased near the pellet periphery. It was reported that the fuels show trends toward increasing degrees of local burnup at the pellet periphery, which causes compositional variations along the radius, and results in the formation of rim zone [8, 9].

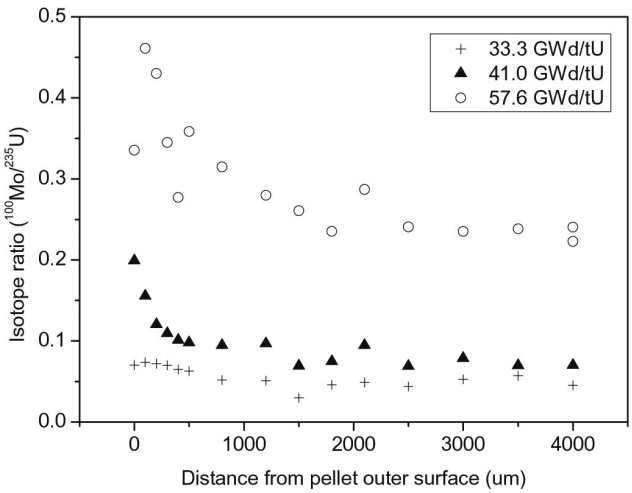

Fig. 1. Distribution of ^{100}Mo Across the Radius of Spent Nuclear Fuels Discharged from Yeonggwang-2 Nuclear Power Plant

Therefore, the increase of Mo content at the pellet periphery could be regarded as the result of high burnup at the periphery (the so-called rim effect). The measured values should be corrected by the estimated isobar effect from ^{100}Ru, which corresponds to ca. 13% of the mass 100 for a spent fuel with 50 GWd/tU. The presence of isobaric ruthenium interference is not discussed here since the profile of distribution is thought to be unchanged and the reproducibility of the measurements was the main concern in this work.

The reproducibility of the isotope ratios was determined by repeating the measurements at the same radial position. Fig. 2 shows the measured values of relative standard deviation (RSD) are 8.6%, 8.6%, and 24% for 33.3, 41.0, and 57.6 GWd/tU specimens, respectively. For the highest burnup, the measured RSD value of the ^{100}Mo/^{235}U ratio was quite large compared to those of the lower burnups, and also as compared to those of the actinide elements which were reported in our previous paper [8]. It is considered that this large deviation is probably derived from the insoluble precipitates which can cause non-uniform distribution in the microscopic region of an ablated crater. To justify this assumption and to ascertain what really happened, the effect of a molybdenum addition on UO_2 fuel was studied in detail.

3.2. Characterization of Mo Mixed UO_2 Pellets

To understand the large deviation of the measured values mentioned above, the molybdenum mixed UO_2 fuels were prepared and the effect of Mo on the phase of UO_2 (face centered cubic, Fm3m) was studied. The molybdenum oxide powder was mixed thoroughly with small size urania particles to ensure homogeneity on a submicrometer scale, and this mixture was then heated to a temperature sufficient to achieve diffusion rates that ensure homogeneity on an atomic level [1]. To understand the status of molybdenum in UO_2 and/or the microstructural transformation of UO_2 by molybdenum, a visual inspection of the prepared pellets was performed by EPMA. Fig. 3 shows the changes of morphology with respect to the Mo content. The pellets maintained a surface morphology of UO_2 for the lowest Mo content, indicating the homogeneity of the Mo distribution, while those with 2 atom% and 4 atom% Mo revealed a lumpy surface, and finally those with the highest content revealed the separated Mo precipitate from the UO_2 matrix. To identify those separated phases from the UO_2 matrix, electron probe micro analysis (EPMA) was carried out. Even though it appears to be homogeneous, it cannot be excluded that there are nanometric metallic precipitants for the sample with the lowest molybdenum content. The microstructures of the samples with the higher molybdenum contents explain the comparatively larger deviation of the ^{100}Mo/^{235}U ratio for the specimens with the highest burnup, as described in section 3.1.

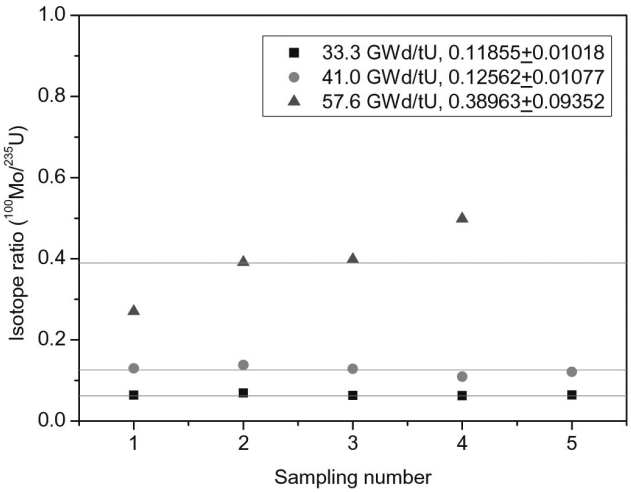

Fig. 2. Reproducibility of ^{100}Mo/^{235}U Ratio of Spent Nuclear Fuel Specimens Measured at the Same Radial Position

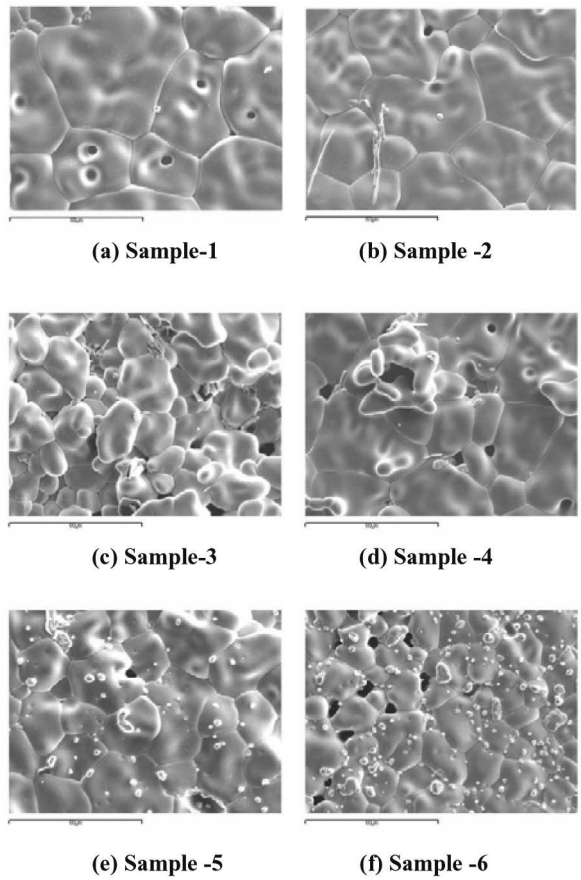

Fig. 3. The Changes of Morphology by Mo Addition on UO_2 Matrix with Respect to Mo Content (atom%): (a) 0%, (b) 1%, (c) 2%, (d) 4%, (e) 8% and (f) 15%

To identify the phases in the prepared urania, powder XRD spectra were obtained. Fig. 4-(a) shows that all these samples have the fluorite structure of UO_2 (cubic, Fm3m), and the samples with high Mo content also show the patterns of Mo. As can be observed in Fig. 4-(b), up to 4 atom% Mo content, the lattice constant of the cubic phase (it was regarded as the $U_{1-x}Mo_xO_2$ phase since no other phases were observed) was increased as the Mo content increased. Above 4 atom% Mo, the lattice constant of the cubic phase was decreased as the Mo content increased, and some Mo did not dissolve into the UO_2 matrix but separated from the UO_2 matrix.

Kleykamp reported that the maximum solubility of molybdenum at 2173 K is below 0.002 mass% Mo and 0.006 mol% MoO_2 [10]. In this experiment, at a glance, the solubility of Mo in the UO_2 matrix seems to be much higher than the previously reported maximum because there are no other phases but molybdenum mixed uranium oxide up to 4% Mo. However, if the molybdenum is dissolved into a UO_2 matrix to form a solid solution, it should have lattice contraction since the ion radius of Mo is smaller than that of uranium [11], and it should also have a linear correlation according to Vegard's law [12]. Therefore, it seems that the changes of lattice parameter up to 4 atom% Mo did not result from the formation of solid solution but from other reasons. Since no other phases but cubic fluorite structure were observed and since unusual changes in the lattice parameters were revealed, it can be

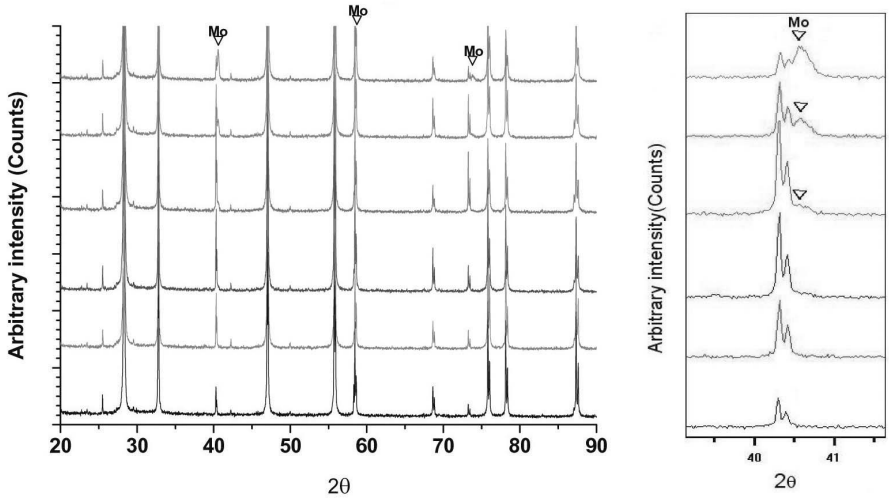

(a) The X-ray diffraction patterns of Mo-added UO_2

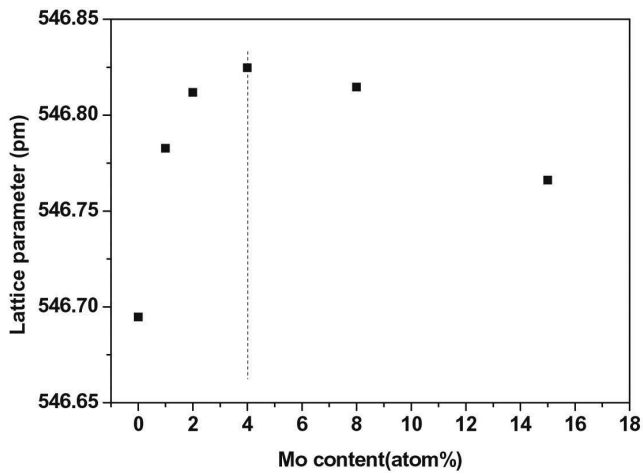

(b) The changes of lattice parameter

Fig. 4. (a) The X-ray Diffraction Patterns of Mo-added UO_2 (Mo Content: 0, 1, 2, 4, 8 and 15 atom% from Bottom to Top, Respectively) and (b) the Changes of Lattice Parameter as a Function of Mo Content

postulated that molybdenum remains in the UO_2 matrix having a fluorite structure associated with a Schottky-type defect. At lower Mo content, although it seems to be homogeneous, the uranium and molybdenum ions are not randomly arranged but rather they cluster together with their own ions to form microscopic-scale, molybdenum-rich regions in a solid solution. This dislike of uranium and molybdenum ions for each other's company, and the segregation of each in the solid solution, seems to cause the small increase in the lattice parameter. For high Mo content, the XRD patterns revealed the contraction of the UO_2 lattice together with the phase separation of Mo metal from the mixed oxide, and the amount of metallic precipitates was increased as the content of molybdenum increased. From the above results, it can be explained that the formation of metallic precipitates is accelerated with increasing Mo content, which causes the removal of Mo from a UO_2 matrix to form the metallic precipitates, which then results in lattice contraction. These results were consistent with those of the EPMA analysis.

From these results, it can be concluded that uranium and molybdenum ions dislike each other, and they cluster together with their own ions to form molybdenum-rich regions even in the solid solution. This segregation of 'like with like' is accelerated with the increase of Mo content, which leads to the decrease of Mo solubility in the UO_2 matrix and results in lattice contraction. The separation of the molybdenum phase from the UO_2 matrix at high Mo content explains the larger deviation of the measured $^{100}Mo/^{235}U$ ratio for the highest burnup due to the non-uniform distribution of Mo in a small scale.

3.3. Oxidation of Mo Added UO_2

Fig. 5 shows the oxidation kinetic curves of molybdenum-added UO_2 by thermogravimetric analysis. The X-ray diffraction spectra for the oxidation of Mo-added UO_2 at 300ºC, 450ºC and 600ºC are shown in Fig. 6. The U-O system could have a complicated oxide phase such as the stable cubic UO_2, U_4O_9, metastable tetragonal U_3O_7, and orthorhombic U_3O_8 [13, 14]. At 300ºC, the temperature corresponding to the first plateau of thermogravimetric curves in Fig. 5(a), UO_2 was oxidized to U_3O_7 and U_3O_8 as shown in the XRD spectrum in Fig. 6(a). Metallic Mo phase was observed for the samples with high Mo content. The intensity of U_3O_8 was decreased

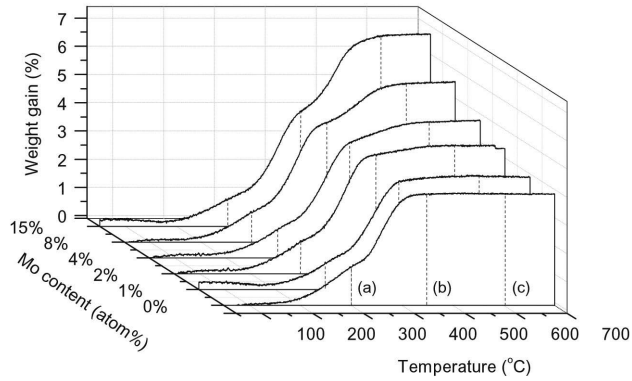

Fig. 5. The Oxidation-kinetic Curves of Mo-added UO_2 by Thermogravimetric Analysis

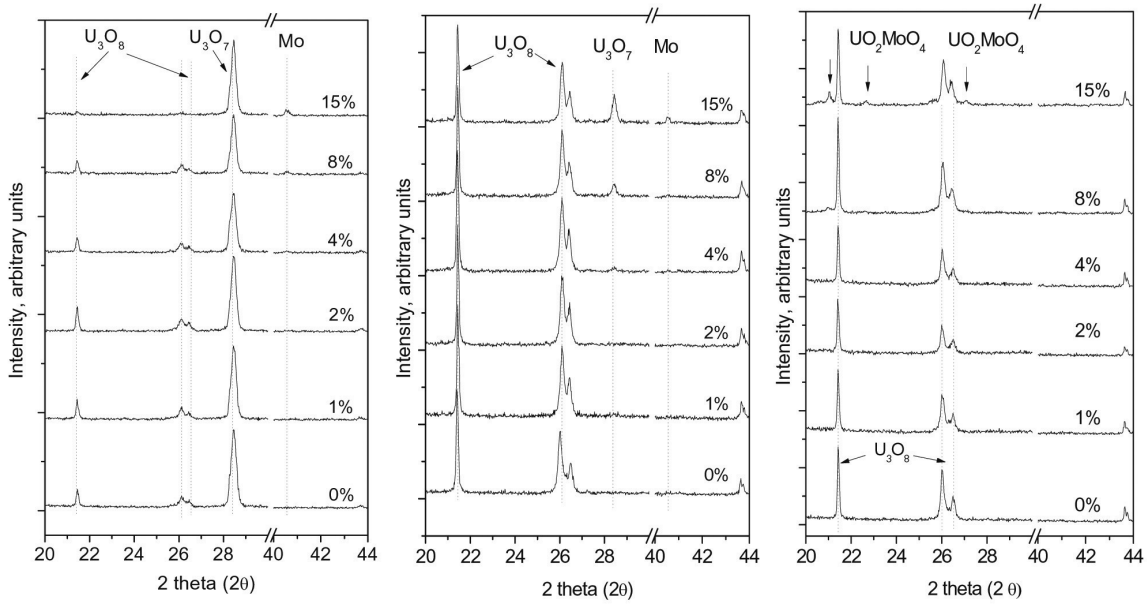

(a) 300°C (b) 450°C (c) 600°C

Fig. 6. XRD Patterns of Mo-added UO_2 after Air Oxidation at (a) 300°C, (b) 450°C, and (c) 600°C for 10 Minutes

as the Mo content increased, indicating the inhibition of oxidation by molybdenum addition. At 450ºC, the temperature corresponding to the second plateau in Fig. 5(b), U_3O_8 was identified as the major phase with a small amount of U_3O_7 phase at the high Mo content. The tendency of the inhibition to UO_2 oxidation by Mo content was confirmed. In addition, metallic Mo phase was also observed for the samples with high Mo content. At 600ºC, the temperature corresponding to the third plateau in Fig. 5(c), UO_2 was oxidized to U_3O_8 completely and another oxidation product was observed which corresponds to monoclinic UO_2MoO_4 phase (Fig 6(c)).

Two different cases can be considered: (a) metallic Mo precipitated in UO_2 matrix, and (b) $(U_xMo_y)O_2$ mixed oxide (solid solution, $x+y=1$) or oxide precipitate as an initial phase. From the existence of metallic Mo up to 450ºC observed by XRD patterns and the amount of weight gains at the second and the third plateaus, we concluded that metallic molybdenum participated in the oxidation reaction in a small way up to 450ºC. It can be postulated that the oxidation reactions of Mo-precipitated uranium oxide proceed as follows.

$$3\,UO_2 + \tfrac{1}{2}O_2 \rightarrow U_3O_7 + \tfrac{1}{2}O_2 \rightarrow U_3O_8 \quad \cdots\cdots\cdots\cdots \quad (1)$$

$$U_3O_8 + 3Mo + 5O_2 \rightarrow UO_2MoO4 \quad \cdots\cdots\cdots\cdots \quad (2)$$

The oxidation reaction of case (a) can be explained by reaction (1) and (2) as described above. The oxidation curves showed the typical two-step reactions of UO_2 oxidation to U_3O_8 (reaction (1)), and then further oxidation with molybdenum to produce UO_2MoO_4 as a next step (reaction (2)). During the first step described in the reaction (1), most of metallic molybdenum was not involved in the UO_2 oxidation. Instead, molybdenum inhibits the oxidation from UO_2 to U_3O_8 by the buffering effect of the Mo/MoO_2 couple. When UO_2 oxidation is completed, the produced U_3O_8 reacts with molybdenum metal and is oxidized to UO_2MoO_4. This observation is incompatible with the oxidation reaction recommended by S. Imoto [15], namely that the main fraction of Mo is more likely to be present in oxide form than as a metal; however, it is compatible to a certain extent with the papers by T. Muromura et al. [16, 17] concerning the partition of Mo between metallic and oxide precipitates.

In the case of mixed oxide (case (b)), the oxidation reaction from $(U_xMo_y)O_2$ mixed oxide ($x+y=1$) may proceed as follows (reaction (3) and (4)). In this work, even though oxide precipitates could exist, we exclude the case because it was hard to find the diffraction patterns of separated oxide phase in the XRD spectrum. During the first step, molybdenum inhibits the oxidation from UO_2 to U_3O_8 as shown in Fig. 6-(a) and (b).

$$3(U_xMo_{1-x})O_2 + \tfrac{1}{2}O_2 \rightarrow (U_xMo_{1-x})_3O_7 + \tfrac{1}{2}O_2 \rightarrow (U_xMo_{1-x})_3O_8 \quad \cdots\cdots\cdots\cdots \quad (3)$$

$$(U_xMo_{1-x})_3O_8 + (1-x)O_2 \rightarrow 3(1-x)UO_2MoO_4 + (2x-1)U_3O_8 \quad \cdots\cdots\cdots\cdots \quad (4)$$

Table 2 compares the calculated weight gains with the measured weight gains for two different cases. At the first step (oxidation up to 450ºC), the measured weight gains were within the range of 4.00±0.17 without any tendency. From the weight gains listed in Table 2, it can be explained that both the metallic precipitate and the mixed oxide are involved in the oxidation reactions. At the second step, for the samples with high Mo-concentration, Mo-precipitated UO_2 seems to be more dominant. In this case, the calculated maximum weight gains (%) at the third plateau are ca. 3.9%, 4.1%, 4.3%, 4.7%, 5.5% and 7.0% for the samples with Mo contents of 0%, 1%, 2%, 4%, 8% and 15%, respectively. The measured weight gains (%) at the third plateau (600ºC) were around 3.8%, 3.9%, 4.4%,

Table 2. Comparison of Weight Gains (%) by Oxidation Reaction Between Mo-precipitated UO_2 and Solid Solution of U-Mo Mixed Oxide

Mo (atom%)	Calculated weight gains (%)				Measured weight gains (%)	
	(a) Metallic Mo in UO_2 matrix		(b) U-Mo mixed oxide			
	1st step	2nd step	1st step	2nd step	1st step	2nd step
0	3.95	3.95	3.95	3.95	3.84	3.85
1	3.93	4.13	3.97	4.09	3.76	3.93
2	3.92	4.32	3.99	4.23	4.15	4.44
4	3.89	4.70	4.04	4.52	4.05	4.70
8	3.83	5.50	4.12	5.11	4.18	5.51
15	3.71	7.00	4.29	6.21	4.06	6.63

4.7%, 5.5% and 6.6% for the samples with 0%, 1%, 2%, 4%, 8% and 15% Mo, respectively. The measured values agreed comparatively well with the calculated values, even though some of them gained a little less weight than expected. Therefore, it can be postulated that the oxidation behavior of Mo-added UO_2 depends on its initial phase; however, all of the added molybdenum participated in the formation of UO_2MoO_4, regardless of the initial phase.

4. CONCLUSION

The distribution of the $^{100}Mo/^{235}U$ ratio in spent nuclear fuels was measured by LA-ICP-MS and the reliability of the values was analyzed by repeating the measurements. As a result, it was observed that Mo is distributed almost constantly in the center of the pellet but it increased near the pellet periphery due to the rim effect depending on the burnup. Concerning reliability, the measured RSD value of the $^{100}Mo/^{235}U$ ratio for the highest burnup was quite large compared to those for the lower burnup, and also with those of the actinide elements reported in our previous paper [6]. According to the results described in this work, the behavior of molybdenum in uranium dioxide can be summarized as follows:

1) The surface morphology of molybdenum-added UO_2 for the lowest Mo content maintained that of pure UO_2, indicating the homogeneity of Mo distribution, while those for 2% and 4 atom% Mo revealed lumpy surfaces, and a phase separation by Mo precipitates was found for the highest content. These microstructures explain the larger deviation of the $^{100}Mo/^{235}U$ ratio for the 57.6 GWd/tU specimens.
2) At molybdenum content lower than 4 atom%, the molybdenum remains in the UO_2 matrix having a fluorite structure associated with a Schottky-type defect. Although it appears to be homogeneous on a macroscopic scale, it seems that the uranium and molybdenum ions are not randomly arranged but that they cluster together with their own ions to form microscopic-scale, molybdenum-rich regions in a solid solution. This causes a small increase in the lattice parameter. At molybdenum contents higher than 4 atom%, there is a tendency to form metallic precipitates since uranium and molybdenum ions dislike each other and the distance between molybdenum particles becomes sufficiently close that the ions segregate from each other as the Mo-concentration increases. The segregation of 'like with like' is accelerated with the increase of Mo content, which leads to the decrease of solubility and which results in a lattice contraction of UO_2 together with the phase separation of molybdenum.
3) Both of the metallic precipitates and the mixed oxide are involved in the oxidation reactions. It seems that the metallic precipitates seem to be dominant for the samples with high Mo-concentration, while mixed oxides (or oxide precipitates) are dominant for the lower Mo-concentration. If Mo is precipitated in the UO_2 matrix, a typical two-step oxidation reaction from UO_2 to U_3O_8 takes place at first. Then, the produced U_3O_8 reacts with Mo to produce UO_2MoO_4 as a next step. In this case, Mo seems to be involved in the oxidation from UO_2 to U_3O_8 in a small way, but it inhibits the UO_2 oxidation.

ACKNOWLEDGEMENTS

This work was supported by a grant from the Nuclear Research & Development Program of the Korea Science and Engineering Foundation (KOSEF), funded by the Korean government (MEST). We also wish to acknowledge the experimental assistance of Mr. Daehyeon Kim.

REFERENCES

[1] P.G. Lucuta, R.A. Verrall, Hj. Matzke and B.J. Palmer, "Microstructural Features of SIMFUEL – Simulated High-burnup UO_2 Based Nuclear Fuel", *Journal of Nuclear Materials*, Vol. 178, p.48 (1991)
[2] H. Kleycamp, "The Chemical State of the Fission Products in Oxide Fuels", *Journal of Nuclear Materials*, Vol. 131, p.221 (1985)
[3] Philippe Martin, Michel Ripert, Gaelle Carlot, Philippe Parent and Carine Laffon, "A Study of Molybdenum Behaviour in UO_2 by X-ray Absorption Spectroscopy", *Journal of Nuclear Materials*, Vol.326, p.132 (2004)
[4] P. Garcia, J.P. Piron and D. Baron, "A Model for the Oxygen Potential of Oxide Fuels at High Burnup", in "Proceedings of Water Reactor Fuel Element Modeling at High Burnup and its Experimental Support", *IAEA-TECDOC-957*, p. 523-538 (1997)
[5] I. Sato, H. Furuya, T. Arima, K. Idemitsu and K. Yamamoto, "Behavior of Metallic Fission Products in Uranium-Plutonium Mixed Oxide Fuel", *Journal of Nuclear Materials*, Vol.273, p.239 (1999)
[6] S. Nicoll, H. Matzke, R.W. Grimes, C.R.A. Catlow, "The Behavior of Single Atoms of Molybdenum in Uranis", *Journal of Nuclear Materials*, Vol.240, p.185 (1997)
[7] E. Walle, P. Perrot, J. Foct, and M. Parise, "Evaluation of the Cs-Mo-I-O and Cs-U-I-O Diagrams and Determination of Iodine and Oxygen Partial Pressure in Spent Nuclear Fuel Rods", *Journal of Physics and Chemistry of Solids*, Vol. 66, p.655 (2005)
[8] Y.-K. Ha, J. Kim, Y.S. Jeon, S.H. Han, H.S. Seo and K. Song, "Local Burnup Characteristics of PWR Spent Nuclear Fuels Discharged from Yeonggwang-2 Nuclear Power Plant", *Nuclear Engineering and Technology*, Vol. 42(1), p.79 (2010)
[9] Hj. Matzke, "On the rim effect in high burnup UO_2 LWR fuels", *Journal of Nuclear Materials*, Vol. 189, 141-148, (1992)
[10] H. Kleykamp, "Solubility of Selected Fission Products in UO_2 and $(U,Pu)O_2$", *Journal of Nuclear Materials*, Vol.206, p.82 (1993)
[11] R.D. Shannon, "Revised Effective Ionic Radii and Systematic Studies of Interatomic Distances in Halides

and Chalcogenides", *Acta Crystallographica*, A 32, p.751, (1976)
[12] A.R. West, "Basic Solid State Chemistry", JOHN WILLEY & SONS, p.253 (1991)
[13] N-J. Cobos, D. Papaioannou, J. Spino and M. Coquerelle, "Phase Characterization of Simulated High Burnup UO_2 Fuel", *J. Alloys and Compounds*, Vol. 271-273, p.610 (1998)
[14] Y.-K. Ha, J.-G. Kim, Y.-J. Park and W.-H. Kim, "Studies on the Air-Oxidation Behavior of Uranium Dioxide; I. Phase Transformation from $(U_{1-y}Gd_y)O_2$ to $(U_{1-y}Gd_y)_3O_8$", *Journal of Nuclear Science and Technology*, Vol. supp. 3, p.772 (2002)
[15] S. Imoto, "Chemical state of fission Products in irradiated UO_2", *Journal of Nuclear Materials*, Vol. 140(1), p.19 (1986)
[16] T. Muromura, T. Adachi, H. Takeishi, Z. Yoshida, T. Yamamoto, K. Ueno, "Metallic Phases Precipitated in UO_2 Fuel: I. Phases in Simulated Fuel", *Journal of Nuclear Materials*, Vol. 151, p.318 (1988)
[17] T. Adachi, T. Muromura, H. Takeishi and T. Yamamoto, "Metallic Phases Precipitated in UO_2 Fuel: II. Insoluble residue in Simulated Fuel", *Journal of Nuclear Materials*, Vol. 160, p.81 (1988)